p16 Gene therapy: A potentially efficacious modality for nasopharyngeal carcinoma

Andrew Wing Cheong Lee,[1,3] Jian-Hua Li,[1,3] Willa Shi,[1,3] Anna Li,[1,3] Emily Ng,[1,3] Ta-Jen Liu,[5] Henry J. Klamut,[1,3] and Fei-Fei Liu[1,2,3,4]

Departments of [1] Experimental Therapeutics and [2] Radiation Oncology, Princess Margaret Hospital/Ontario Cancer Institute, University Health Network, Toronto, Ontario, Canada; Departments of [3] Medical Biophysics and [4] Radiation Oncology, University of Toronto, Toronto, Ontario, Canada; and [5] Department of Neuro-Oncology, M.D. Anderson Cancer Center, University of Texas, Houston, TX

Abstract

p16 is an important regulator of the cell cycle at the G_1 phase. Frequent aberration of *p16* in nasopharyngeal carcinoma (NPC) suggests a role for this tumor suppressor gene in disease development. *p16* gene transfer has been demonstrated to be effective in various human cancer models, including breast, lung, and prostate, causing cell cycle arrest, apoptosis, and tumor growth delay. We investigated the potential of adenoviral-mediated *p16* therapy, in combination with ionizing radiation (RT), in two distinct NPC models. Two ΔE1 adenoviral vectors were employed: one carrying the human *p16* gene (adv.*p16*), and the other a β-*galactosidase* reporter gene (adv.β-*gal*), both driven by the cytomegalovirus (CMV) promoter. Two NPC cell lines with differential endogenous p16 expression, CNE-1 (low) and CNE-2Z (high), were evaluated for protein expression, cytotoxicity, cell cycle analysis, apoptosis, and senescence. The CNE-1 cells were exquisitely sensitive to adv.*p16*, with 0.1% survival level after gene therapy [25 plaque-forming unit (pfu)/cell], which further decreased to 0.01% with the addition of RT (2 Gy). This reduction in survival was effected through necrosis, G_1 arrest, and senescence. In contrast, CNE-2Z cells were resistant to adv.*p16* gene transfer, with 75% surviving at an equivalent viral dose. This differential sensitivity was recapitulated *in vivo* in that adv.*p16*-treated CNE-1 cells formed no tumors in severe-combined-immunodeficiency (SCID) mice, followed for over 100 days. In contrast, tumor formation was detected 40 days after implantation of adv.*p16*-treated CNE-2Z cells. In conclusion, adv.*p16* gene transfer appears to be highly effective against NPC that lack functional p16, which is the situation in the majority of NPC patients. (Mol Cancer Ther. 2003;2:961–969)

Received 10/21/02; revised 4/9/03; accepted 7/17/03.

The costs of publication of this article were defrayed in part by the payment of page charges. This article must therefore be hereby marked advertisement in accordance with 18 U.S.C. Section 1734 solely to indicate this fact.

Grant support: The Canadian Institutes of Health Research, the Elia Chair in Head/Neck Cancer Research, and the NSERC.

Requests for Reprints: F-F. Liu, Department of Radiation Oncology, Princess Margaret Hospital/Ontario Cancer Institute, 610 University Avenue, Toronto, Ontario, M5G 2M9 Canada. Phone: (416) 946-2123; Fax: (416) 946-4586. E-mail: Fei-Fei.Liu@rmp.uhn.on.ca

Introduction

Nasopharyngeal carcinoma (NPC) is a malignancy of the head and neck region. It is endemic in many geographical regions, including southern China and Southeast Asia (1), and affects a relatively young population (2). Potential etiological factors found to be associated with NPC include EBV infection, environmental factors, and genetic susceptibility (3). Despite the high rates of local tumor control achieved with complex radiotherapy (RT) techniques, NPC is still associated with a significant risk of distant metastases (4). The overall 5-year survival rate is approximately 65% (5), indicating a need for novel therapeutic strategies that may improve patient outcome.

Allelic loss on chromosome 9 has been frequently observed in NPC (61% of primary tumors) (6), particularly at 9p21–22, where *p16* is located. p16 is a regulator of the G_1 phase of the cell cycle; progression through the cell cycle is dependent on the orderly activation of various complexes of cyclins and cyclin-dependent kinases (CDK). It is the CDK4- or CDK6-cyclin D complex that is particularly crucial for the early transition from G_1 to S phase. As a member of the INK4 family (*In*hibitor of CD*K4*), p16 competes with cyclin D for CDK4 or 6 binding. This results in inhibition of CDK activity, leading to G_1 arrest (7). *p16* inactivation is a common event in NPC (60–80% of primary tumors), and may thus play an important role in disease progression (6).

In NPC, *p16* can be inactivated through multiple mechanisms, including homozygous deletion, promoter hypermethylation, and point mutation (6, 8–12). Therefore, selective replacement of *p16* offers a potentially attractive strategy to correct the malignant phenotype. Adenoviral-mediated *p16* gene transfer (adv.*p16*) has been evaluated in several other human cancer models, including head and neck (13), breast (14), lung (15), prostate (16), and pancreas (17). These studies consistently demonstrate that cancers null for *p16* status were highly sensitive to p16 gene transfer (18–21), with evidence of growth inhibition, apoptosis, and tumor suppression (21). Together, these results indicate that *p16* gene transfer, in combination with conventional therapy, may be particularly effective in treating NPC.

In this study, we examine the contribution of adenoviral-mediated *p16* gene transfer to the therapeutic benefit of RT in two NPC cell lines that differ in their endogenous p16 status. We demonstrate that this therapeutic strategy is highly effective against the cell line that lack p16 function.

Downloaded from http://aacrjournals.org/mct/article-pdf/2/10/961/1864970/961-969.pdf by guest on 05 October 2024

Materials and Methods

Cells and Culture Conditions

Two distinct NPC cell lines, CNE-1 (22) and CNE-2Z (23), were obtained from the Cancer Institute/Chinese Academy of Medical Sciences in China. Both cell lines were maintained in αMEM supplemented with 10% v/v fetal bovine serum (FBS). Both cell lines harbor a point mutation in the splice acceptor site of exon 2 of *p16* in the second base (A to C) (12). However, our sequencing data suggested that CNE-2Z cells harbor a heterozygous mutation for the *p16* gene (data not shown).

The human embryonic kidney (HEK) 293 and cervix HeLa cell lines (American Type Culture Collection) were also used in the study. Both cell lines were maintained in αMEM containing 10% FBS.

Recombinant Adenoviral Vectors

Ad5CMV-*p16* (adv.*p16*) is a replication-deficient adenoviral vector containing a cytomegalovirus (CMV) promoter upstream of the human wild-type *p16* gene (from Dr. T-J.Liu). A control adenoviral vector, Ad5CMV-*β-gal* (adv.*β-gal*) expressing the *β-galactosidase* reporter gene, was kindly provided by Dr. F. Graham of McMaster University (Hamilton, Canada).

Both adenoviral vectors were propagated in HEK 293 cells, purified by cesium chloride (CsCl) density gradients, and titered using plaque-forming assay (24, 25). Purified adenoviral vectors were also examined for revertant adenoviruses through consecutive rounds of infection using HeLa cells as previously described (25).

In Vitro Adenoviral Infection

All *in vitro* infections were performed by adding an appropriate volume of the purified and titered adenovirus (adv.*p16* or adv.*β-gal*) to cells, along with a small volume of αMEM containing 2% v/v heat-inactivated FBS. Infections were conducted for 1 h at 37% in 5% CO_2, and were completed by adding αMEM (10% FBS) directly to each flask. Iso-equivalent viral doses were used for CNE-1 and CNE-2Z infections by conducting β-galactosidase assays as previously described (25) to normalize transduction efficiency differences between the two cell lines. Hence, adenoviral doses of 5, 10, or 15 plaque-forming unit (pfu)/cell in CNE-1 cells were iso-equivalent to 17, 34, or 70 pfu/cell for CNE-2Z cells.

Clonogenic Assays

After adv.*p16* infection (at 0, 5, 10, and 25 pfu/cell CNE-1 iso-equivalent doses) and/or 2 Gy of RT administered 24 h later, CNE-1 or CNE-2Z cells were trypsinized and counted. Subsequently, 10^2–10^5 cells were plated onto 100 mm^2 dishes (Nunc, Denmark), and grown in αMEM with 10% FBS at 37°C/5% CO_2. Colonies were subsequently fixed and stained with methylene blue (in 50% ethanol). Triplicate dishes were set up for each condition, and each experiment was repeated at least twice.

Western Blot Analysis

Approximately 1×10^6 CNE-1 or CNE-2Z cells (infected or irradiated) in T25 flasks were rinsed with PBS and harvested in lysis buffer [0.1 M Tris-Cl (pH 8.0), 1% SDS, 10 mM EDTA, and 2 mM DTT]. Samples containing equal amounts of protein were run on SDS-PAGE gels [8% for retinoblastoma protein (pRb), 12% for p16 and β-actin] for 90–120 min at 110 V, and transferred onto nitrocellulose membranes (at 15 V for 30 min). Blots were then probed using the respective primary antibodies in 0.1% PBST containing 5% milk [1.5 μg/ml p16 monoclonal antibody (mAb) (NeoMarkers, Fremont, CA); 1 μg/ml pRb mAb (PharMingen, San Diego, CA); and 1:1000 working dilution of β-actin mAb (Sigma, St. Louis, MO)]. After several washings with 0.1% PBST, the blots were incubated with a horseradish peroxidase-conjugated secondary antibody (Amersham, Piscataway, NJ). Anti-mouse secondary Ab was used against both p16 and pRb mAb, whereas an anti-rabbit secondary Ab was used against the actin mAb. Proteins of interest were visualized using a chemiluminescence reagent (Santa Cruz Biotechnology, Santa Cruz, CA). Y79 is a retinoblastoma cell lysate used as a positive control for p16 protein and a negative control for pRb (kindly provided by Dr. B. Gallie, OCI). A549 is a non-small cell lung cancer cell line (kindly provided by Dr. M. Tsao at OCI) serving as a negative control for p16, and a positive control for pRb.

Cell Cycle Analysis Using Flow Cytometry

Twenty-four or 48 h after infection (2 pfu/cell of either adv.*p16* or adv.*β-gal*), or irradiation (2 Gy), $1–3 \times 10^6$ CNE-1 or CNE-2Z cells were pelleted and fixed with 4 ml of ice-cold 70% ethanol added dropwise. Ethanol was removed, washed with PBS twice, and then the cell pellets were resuspended in 500 μl of buffer (0.2% Triton X-100, 1 mM EDTA in PBS). The suspension was then treated with 50 μg/ml of RNaseA, and stained with 50 μg/ml of propidium iodide at room temperature for 60 min. Cell cycle analysis was performed on an EPICS analyzer using ModFit LT2.0 software (Beckman Coulter, Fullerton, CA). Each experiment was performed three times. The *P*-value was obtained using the Student *t* test by comparing treated samples (adv.*β-gal*, adv.*p16*, or irradiated) with control (uninfected) for each phase of the cell cycle.

Senescence-Associated *β*-Galactosidase Staining

CNE-1 cells (1.5×10^5) were transferred onto six-well plates and grown for 2 days. Subsequently, they were infected with adv.*p16* (5, 10, 15, or 25 pfu/cell) for 24, 32, or 48 h. After those set times, cells were washed twice with PBS and fixed with 2% formaldehyde/0.2% glutaraldehyde for 10 min at 4°C. Cells were then incubated with staining solution (consisting of X-gal solution buffered to pH 6.0 with citric acid/sodium hydrogen phosphate) for 24–48 h at 37°C. Senescent cells with detectable SAB will turn blue, and the number of such cells was counted under a microscope. Infection by adv.*β-gal* provided negative controls.

Morphological Assessment of Apoptosis and Necrosis

Cell death was evaluated morphologically using acridine orange-ethidium bromide (AO-EB) (Sigma) fluorescence staining. CNE-1 cells were assayed 2 days following infection with adv.*β-gal* (60 pfu/cell) or adv.*p16* (60 pfu/

Downloaded from http://aacrjournals.org/mct/article-pdf/2/10/961/1864970/961-969.pdf by guest on 05 October 2024

cell), or 24 h after irradiation (2 Gy). They were washed with PBS, pelleted at 1300 rpm, resuspended in a small amount of PBS, and then mixed with 20 μl of AO-EB stock to a final concentration of 2.5 μM. A small volume of stained cells was placed onto glass slides and immediately visualized using fluorescence microscopy (Leica, Switzerland). The assay allows morphological inspection, as well as quantification of cells undergoing either apoptosis or necrosis. For each slide, nine fields of view containing at least 200 cells were counted. The level of apoptosis or necrosis for each treatment condition was determined from three independent experiments. By comparing infected or irradiated cells with untreated samples, *P*-values were determined using the Student *t* test.

DNA Fragmentation Assay

CNE-1 cells were treated under various conditions: mock infection; adv.*p16* (25 pfu/cell); adv.*p53* (50 pfu/cell); or adv.*β-gal* (25 pfu/cell). Genomic DNA was extracted 2 days after infection using the Puregene DNA isolation kit (Gentra Systems, Minneapolis, MN) and then subjected to gel electrophoresis at 100 V in a 1.8% agarose gel. Cells treated with adv.*p53* (50 pfu/cell) provided a positive control for apoptosis (25, 26). Cells subjected to four rounds of freezing (−70°C) and thawing (37°C) provided the positive control for necrosis (27).

Tumor Formation Experiments

CNE-1 or CNE-2Z cells were treated with adv.*β-gal* (25 pfu/cell) or adv.*p16* (25 pfu/cell), and 24 h later, were trypsinized and injected into the left gastrocnemius muscle of severe-combined-immunodeficiency (SCID) mice. About 4×10^6 cells resuspended in 100 μl of PBS were injected into each animal. Another set of experiments was conducted, whereby 75% of the injected CNE-1 cells were infected with adv.*p16* (3×10^6 infected cells were mixed with 1×10^6 uninfected cells before each injection). Each experiment was repeated twice, and at least two animals were used for each infection condition. Animals were monitored twice a week for tumor formation by measuring the leg plus tumor diameter, which was later converted to tumor weight as previously described (28). Mean tumor weight ± SE was then calculated for each time point. The mice were sacrificed for humane reasons once the tumor burden was judged to be excessive. These experiments are conducted in accordance with guidelines set by the University Health Network Animal Ethics Board.

Results

Endogenous p16 and pRb Status of CNE-1 and CNE-2Z Cells

Before evaluating the therapeutic effect of adv.*p16*, basal expression levels of p16 and pRb in the two NPC cell lines were evaluated. In CNE-1 cells, p16 expression was virtually undetectable (Fig. 1A), which is in contrast to CNE-2Z cells, where high levels of endogenous p16 expression were observed (Fig. 1B). Both cell lines, however, expressed high levels of pRb.

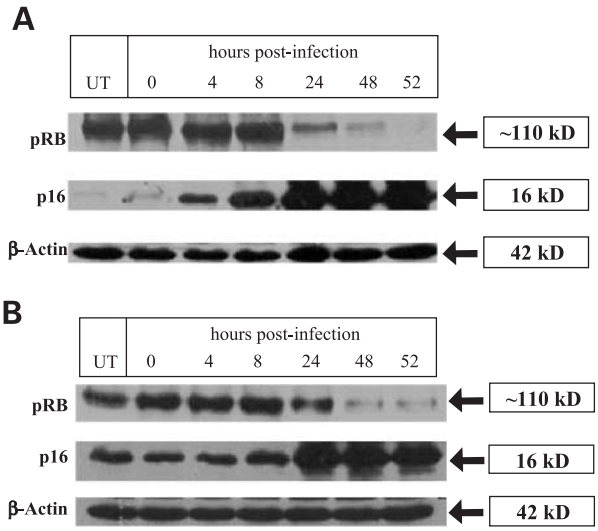

Figure 1. **A,** kinetics of p16 and pRb expression in CNE-1 cells infected with adv.*p16*. Western blot analysis revealed an increase in p16 expression detectable at 4 h following adv.*p16* infection (5 pfu/cell). Lysed protein (20 μg) was resolved on SDS-PAGE gels (8% for pRb; 12% for p16 and β-actin loading control), as described in ''Materials and Methods.'' *UT,* untreated CNE-1 cells. **B,** kinetics of p16 and pRb expression in CNE-2Z cells infected with adv.*p16*. CNE-1 iso-equivalent viral dose (17 pfu/cell) was used in this experiment. An increase in p16 expression was most apparent 24 h after adv.*p16* infection. Lysed protein (20 μg) was loaded onto SDS-PAGE gels, and immunoblotting was performed as described in ''Materials and Methods.'' *UT,* untreated cells.

Kinetics of p16 and pRb Expression following adv.*p16* Infection

Western blot analysis demonstrated that recombinant p16 could be detected in CNE-1 cells 4 h following adv.*p16* infection (5 pfu/cell) (Fig. 1A). p16 expression continued to increase until 48–52 h postinfection. An inverse relationship was observed between p16 and pRb in that as p16 expression increased, pRb levels decreased correspondingly.

In contrast to CNE-1 cells, p16 kinetics appeared to be delayed in the CNE-2Z cells (Fig. 1B). No further increase in p16 expression was detected until 8–24 h after adv.*p16* infection using iso-equivalent viral doses.

Our objective was to combine adv.*p16* therapy with RT, hence it was important to examine the effect of RT on recombinant p16 expression. Independent of *p16* gene transfer, RT (2 Gy) had no influence on endogenous or recombinant p16 expression in either cell line (Fig. 2). Interestingly, RT appeared to enhance the level of total pRb in CNE-1 cells under both uninfected and infected conditions (Fig. 2A). Similarly, RT alone appeared to increase the expression of total pRb in CNE-2Z cells (Fig. 2B). The increase in p16 expression following adv.*p16* treatment might have counteracted the pRb up-regulation caused by RT in both cell lines (Fig. 2).

Cytotoxic Effect of adv.*p16* on CNE-1 and CNE-2Z Cells

Clonogenic assays were performed to determine the sensitivity of CNE-1 and CNE-2Z cells to adv.*p16* gene

Downloaded from http://aacrjournals.org/mct/article-pdf/2/10/961/1864970/961-969.pdf by guest on 05 October 2024

transfer, in combination with RT (2 Gy). CNE-1 cells were infected using a range of adv.*p16* doses from 0 to 25 pfu/cell. As indicated in Fig. 3, *p16* gene transfer alone caused significant cytotoxicity to CNE-1 cells, resulting in a surviving fraction of only 0.1% with adv.*p16* at 25 pfu/cell. In contrast, CNE-2Z cells were resistant at iso-equivalent viral doses, displaying a similar response to that induced by the vector control (adv.*β-gal*) (data not shown). At an iso-equivalent dose of 15 pfu/cell, adv.*p16* was approximately 100-fold more cytotoxic to CNE-1 than CNE-2Z cells.

On the basis of the parallel slopes of the survival curves (with or without RT), RT at 2 Gy appeared to contribute to the cytotoxicity of adv.*p16* in an additive manner for both cell lines, causing a further 10-fold reduction of survival in CNE-1 cells.

Examination of Modes of Cytotoxicity in CNE-1 Cells

In light of the impressive cytotoxic effects observed in the CNE-1 cells after adv.*p16* gene transfer, we proceeded to examine the possible modes of death in these cells.

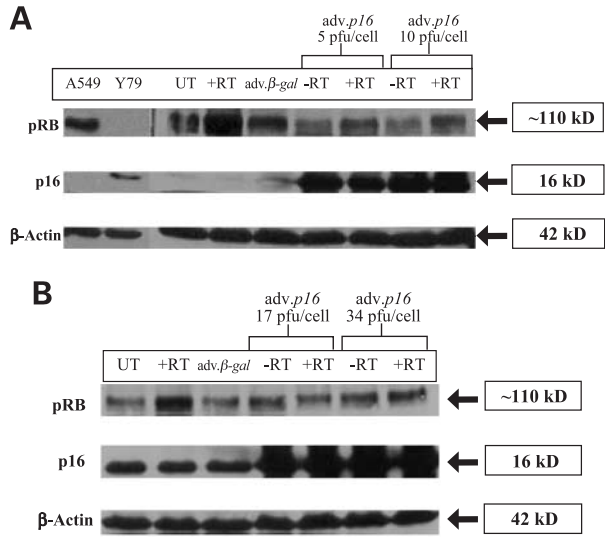

Figure 2. **A,** p16 and pRb protein levels in CNE-1 cells treated with adv.*p16* ± RT. Twenty-four hours after infection, cells were irradiated (2 Gy). Cell lysates were collected the following day and immunoblotting was performed. No detectable change in p16 expression was observed 24 h following RT (2 Gy). RT increased pRb levels in the cells. *Lane assignments: lane 1,* A549 (pRb-positive/p16-negative control); *lane 2,* Y79 (pRb-negative/p16-positive control); *lane 3,* untreated CNE-1 cells (*UT*); *lane 4,* RT alone (2 Gy); *lane 5,* adv.β-*gal* (10 pfu/cell); *lanes 6 and 7,*adv.*p16* (5 pfu/cell) ± 2 Gy; *lanes 8 and 9,* adv.*p16* (10 pfu/cell) cell) ± 2 Gy. Lysed protein (20 μg) was resolved on an 8% SDS-PAGE gel for pRb, and 12% for p16 and β-actin loading control, and Western blotting was performed as described in ''Materials and Methods.'' **B,** p16 and pRb protein levels in CNE-2Z cells treated with adv.*p16* ± RT. Same experimental condition as in Fig. 3. RT (2 Gy) had little effect on p16 expression 24 h after treatment. In *lane 2*, RT alone appears to have increased pRb expression. *Lane assignments: lane 1,* untreated CNE-2Z cells; *lane 2,* RT alone (2 Gy); *lane 3,* adv.β-*gal* (34 pfu/cell); *lanes 4 and 5,* adv.*p16* (17 pfu/cell) ± 2 Gy; *lanes 6 and 7,* adv.*p16* (34 pfu/cell) ± 2 Gy. Lysed protein (20 μg) was resolved on SDS-PAGE gels and immunoblotting was performed as described in ''Materials and Methods.''

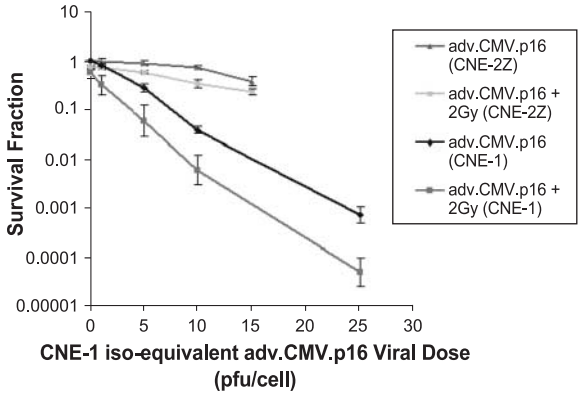

Figure 3. Clonogenic survival of CNE-1 and CNE-2Z cells following adv.*p16* ± RT. Twenty-four hours after infection with adv.*p16*, cells were irradiated (2 Gy), counted, and plated in triplicate to determine surviving fraction. Iso-equivalent viral doses were used for CNE-2Z cells. *Points,* mean of at least three independent experiments; *bars,* SE.

Adenoviral-mediated *p16* gene transfer has been demonstrated to block cell proliferation in various cancer models (14, 21, 29, 30). To determine the effect of p16 overexpression on cell cycle distribution, CNE-1 and CNE-2Z cells were treated with either adv.*p16* infection (2 pfu/cell) or RT (2 Gy), and then examined by propidium iodide flow cytometry 24 or 48 h later. A 10% increase in the proportion of cells in the G_0-G_1 phase relative to untreated or adv.*β-gal*-infected cells was observed after adv.*p16* therapy (from 62% to 72%) (Fig. 4A). G_1 arrest occurred concurrently with a reduction in the percentage of S-phase cells. RT alone perturbed the cell cycling slightly with a higher proportion in the G_2-M phase.

We could not detect any effect of adv.*p16* infection on cell cycle at 48 h because by this time, the cells have become confluent, with >85% of control cells already in the G_0-G_1 phase (data not shown). CNE-2Z cells were also examined for possible changes in cell cycling as a result of adv.*p16* treatment. As can be observed in Fig. 4B, no changes were detected in these cells as a result of either adv.*p16* or adv.*β-gal* infection, although RT had a similar effect as with the CNE-1 cells.

Numerous studies have demonstrated that p16 overexpression can facilitate premature senescence in both transformed and non-transformed cells (31–35). One striking effect of adv.*p16* therapy on the CNE-1 cells is the change in morphology characterized by increased cell size and flattening, reminiscent of cellular senescence. One biochemical feature of senescence is the expression of SAB. Twenty-four hours following adv.*p16* infection (15 pfu/cell) of CNE-1 cells, SAB activity was detected, suggesting that p16 can induce senescence in NPC cells (Fig. 5, A and B). There was evidence of both a time- and dose-dependent increase in the absolute number of SAB-expressing cells after treatment with adv.*p16* (Fig. 5C). However, the proportion of SAB-expressing cells remained at less than 10%, suggesting that senescence may not play a major role in adv.*p16*-induced cytotoxicity of CNE-1 cells.

Downloaded from http://aacrjournals.org/mct/article-pdf/2/10/961/1864970/961-969.pdf by guest on 05 October 2024

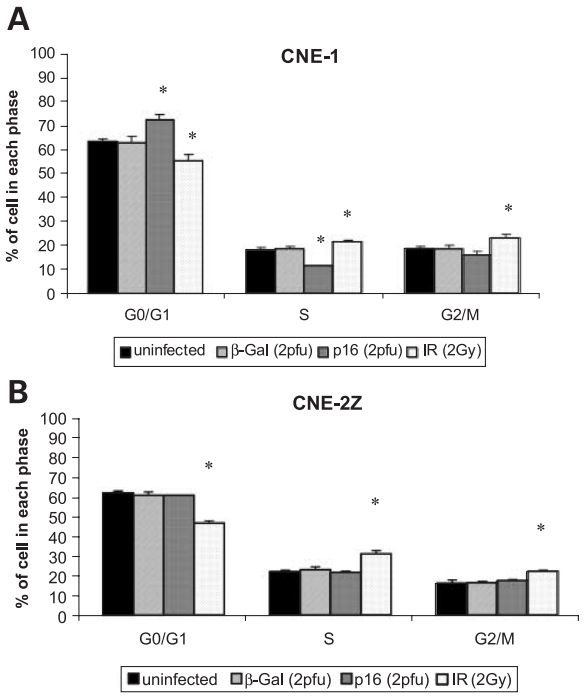

Figure 4. Cell cycle analysis of CNE-1 (**A**) or CNE-2Z (**B**) cells following adv.β-*gal* and adv.*p16* infection or RT. Cell cycle distribution was obtained by staining cells with 50 μg/ml of propidium iodide at room temperature for 30 min. The data were analyzed on an EPICS analyzer using the ModFit LT2.0 software. *Columns,* mean from a minimum of three independent experiments; *bars,* SD. Changes in the cell cycle distribution compared cells treated with adv.β-*gal*, adv.*p16*, or RT (*IR*), to the untreated sample; *asterisks* denote statistically significant differences ($P < 0.05$).

Many investigators have reported that p16 overexpression can induce apoptosis and necrosis in several human cancer models (16, 17, 20, 30, 36–38). To determine whether these processes contribute to p16 cytotoxicity in CNE-1 cells, cells were stained with AO-EB 48 h after adv.*p16* infection, and/or 24 h after RT (2 Gy). Cell viability was determined by the differential uptake of the two fluorescent DNA-binding dyes: AO (green) and EB (orange). Treated cells were analyzed and counted, and the data are summarized in Table 1.

Twenty-four hours after CNE-1 cells were treated with RT, morphological changes associated with apoptosis were observed (Fig. 6A). Treatment of CNE-1 cells with adv.*p16* (60 pfu/cell) resulted in significant induction of necrosis (20%) (Fig. 6B and Table 1).

DNA fragmentation was performed as an alternate assay to corroborate the modes of cell death determined by AO-EB staining. Two days following treatment of CNE-1 cells with adv.*p16* (25 pfu/cell), the DNA agarose gel displayed a combination of both smearing and nuclear fragmentation, with smearing apparently being more prominent (Fig. 7). While DNA smearing is a feature of necrosis (DNA is extensively degraded) (27), DNA laddering is an indication that cells are undergoing apoptosis. Together, these data demonstrate that adv.*p16*-infected CNE-1 cells undergo both necrosis and apoptosis, with the former perhaps playing a more important role than the latter.

adv.*p16* Inhibits Tumor Formation of CNE-1 Cells

The impact of adenoviral-mediated *p16* gene transfer on tumor formation was assessed for both CNE-1 and CNE-2Z cells *in vivo*. Approximately 4×10^6 cells (untreated, infected with adv.*β-gal* or adv.*p16*) were injected into the gastrocnemius muscle of SCID mice 24 h after *in vitro* infection. Mice given injections of mock or adv.*β-gal*-infected CNE-2Z cells were sacrificed at 60–70 days due to tumor burden. In addition, tumor formation was consistently detected for the CNE-2Z cells infected with adv.*p16* (Fig. 8A).

In contrast, for the mice given injections of CNE-1 cells treated with 100% adv.*p16* (25 pfu/cell), no tumors ever formed, even after monitoring for over 100 days (Fig. 8B). Interestingly, for the mice given injections of 75% of the CNE-1 cells having been infected with adv.*p16* (25 pfu/cell),

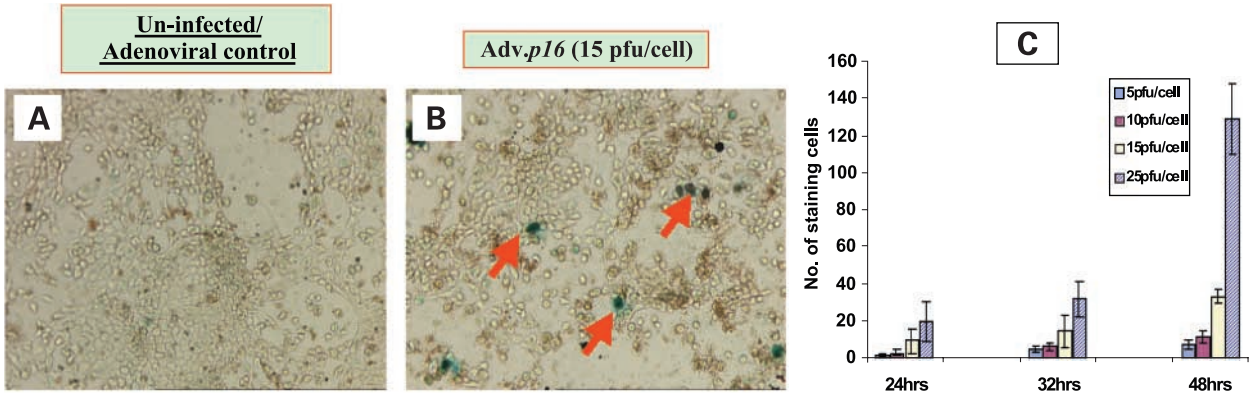

Figure 5. SAB staining of CNE-1 cells infected with adv.*p16*. Photomicrograph of SAB-expressing cells: uninfected (**A**); 24 h after infection (15 pfu/cell) whereby *dark blue* (*red arrows*) cells are indicative of SAB expression; magnification, 100× (**B**); plot of increasing number of SAB-expressing cells as a function of time (24, 32, or 48 h postinfection) and dose (5, 10, 15, or 25 pfu/cell) (**C**).

Downloaded from http://aacrjournals.org/mct/article-pdf/2/10/961/1864970/961-969.pdf by guest on 05 October 2024

Table 1. Apoptosis and necrosis in CNE-1 cells after adv. *p16* ± RT

	% Apoptosis	% Necrosis
Uninfected	21 ± 2	0 ± 0
2 Gy RT	25 ± 2	1 ± 1
adv.*ß-gal* (60 pfu/cell)	21 ± 4	3 ± 0
adv.*p16* (60 pfu/cell)	16 ± 1	18 ± 5*
adv.*p16* + 2 Gy (60 pfu/cell)	16 ± 2	20 ± 7*

Note: Summary of morphological assessment of CNE-1 cells treated with adv.*p16* ± RT. Twenty-four hours after infection with adv.*p16* (60 pfu/cell), CNE-1 cells were irradiated (2 Gy). One day after RT, the cells were stained with AO-EB to assess apoptosis or necrosis. RT alone induced minimal apoptosis ($P < 0.07$). However, significant necrosis was observed following adv.*p16* ± RT. Each value represents the mean ± SD of at least three experiments. The P-value ($^*P < 0.04$) was calculated by comparing the treated cells (adv.*p16* ± RT) with the untreated sample.

with the other 25% uninfected, tumors were still detectable by 40 days postinjection. This result indicates that close to 100% tumor transduction *in vivo* is necessary, to achieve complete tumor cure.

Discussion

The results presented in this study provide important evidence that adenoviral-mediated *p16* gene transfer induces significant cytotoxicity in NPC cells lacking p16 function. Sensitivity is strongly correlated with level of endogenous p16, being most effective in cells with undetectable p16 expression under basal conditions.

On the basis of our previous extensive experience with CNE-1 and CNE-2Z cells, these two NPC cell lines share identical *p53* mutations and display similar morphological features. In addition, they exhibited comparable sensitivity to various treatment modalities, including RT, adv.*p53* gene therapy, and hyperthermia (25, 26, 39). Therefore, their disparate p16 kinetics and sensitivity to adv.*p16* treatment is almost certainly related to their distinct endogenous p16 expression. This correlation is corroborated by other reports in the literature (14, 19–21) concerning adv.*p16* efficacy in other human cancer models.

The differential sensitivity of cancer cells to gene transfer being associated with the endogenous level of the targeted gene has been previously documented. This is particularly evident with adv.*p53* therapy, wherein cells that are null or mutant for *p53* were far more sensitive to exogenous *p53* therapy than cells harboring the wild-type gene (40, 41). Although the precise mechanism behind this finding remains unclear, it might reflect a homeostatic balance between cancer cell survival and apoptosis (40–43). Specifically, if the proliferation or survival signal of a cancer cell were dependent on the mutational defect of a specific gene, it is conceivable that introduction of the wild-type gene into the cell will perturb the fine balance of pro- and anti-proliferative signals, sensitizing the cancer cell toward death. In contrast, introducing a therapeutic gene that was normally expressed or regulated in a cancer cell would be expected to cause minimal effect on cell survival (40, 41).

However, because these two NPC cell lines are non-isogenic, a definitive conclusion relating to endogenous p16 status cannot be drawn. There may be a myriad of other genetic differences that influence sensitivity to adv.*p16* therapy. Nevertheless, until such factors have been elucidated, endogenous p16 status appears to closely correlate with sensitivity to adv.*p16*-mediated cytotoxicity.

The inverse relationship between p16 and pRb expression in both NPC cell lines (Fig. 1) is consistent with previous evidence demonstrating that p16 is capable of down-regulating pRb expression at the transcriptional level (16, 44). Therefore, the decline in pRb protein levels by 24 h post-adv.*p16* infection (Fig. 1) likely reflects an earlier decline in pRb mRNA levels and normal turnover of the pRb protein (half-life > 8 h) (45). However, the possibility that p16 also affects the half-life of pRb cannot be formally excluded without further experimentation. It is conceivable that p16 and pRb could counterbalance each other, to maintain cell cycle regulation. It has been reported that if pRb expression were unresponsive to p16 regulation, p16 would lose its ability to inhibit cell cycle progression (46).

The combination of adv.*p16* and RT resulted in an additive cytotoxic interaction in both NPC cell lines (Fig. 3). Because other groups have reported that *p16*-induced radiosensitization is a *p53*-dependent event (47, 48), and that both cell lines are heterozygous mutants for *p53*, it is

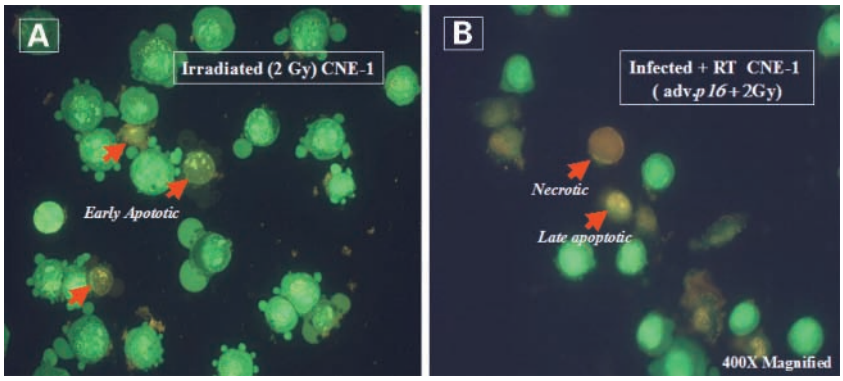

Figure 6. Morphological analysis of apoptosis and necrosis in CNE-1 cells. **A,** after CNE-1 cells were irradiated (2 Gy), an increase in early apoptotic cells was observed. **B,** when RT was combined with adv.*p16*, a significant number of cells underwent necrosis. Magnification, 400×.

Downloaded from http://aacrjournals.org/mct/article-pdf/2/10/961/1864970/961-969.pdf by guest on 05 October 2024

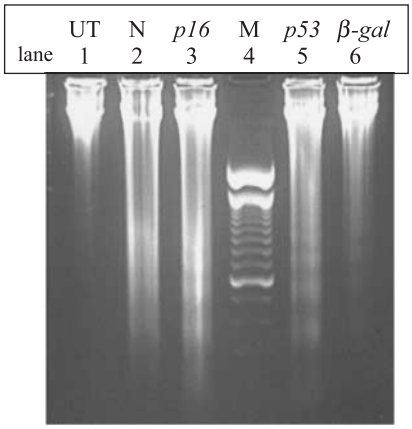

Figure 7. DNA laddering and smearing in CNE-1 cells post-adv.*p16* infection. DNA was extracted 48 h after each treatment. *Lane assignments: lane 1,* untreated cells (*UT*); *lane 2,* necrotic positive control (*N*); *lane 3,* adv.*p16* (25 pfu/cell); *lane 4,* 100 bp DNA marker; *lane 5,* adv.*p53* (50 pfu/cell); *lane 6,* adv.β-*gal* (25 pfu/cell). Necrosis was induced by four rounds of freezing and thawing, rendering a random smearing pattern of the DNA.

predicted that RT-mediated cytotoxicity for our NPC model would be merely additive. Introduction of wild-type *p53* to our NPC cell lines before adv.*p16* infection would allow us to address the issue of p16/p53-mediated radiosensitization, which could be a subject for future studies.

To elucidate the biological impact of exogenous *p16* on CNE-1 cells, various modes of cytotoxicity were examined, including cell cycle arrest, senescence, apoptosis, and necrosis. Our results indicate that adv.*p16*-mediated effect is likely multimodal in its contribution to cytotoxicity and tumor suppression. The increase in G_0-G_1 arrest in CNE-1 cells following *p16* gene transfer clearly validates p16 as an important G_1 checkpoint regulator. Similar results have already been reported, whereby stable transfection of *p16* into CNE-1 cells led to significant G_1 arrest (49). In contrast to adv.*p16*, RT induced G_2-M arrest in both CNE-1 and CNE-2Z cells. A number of molecular changes might have occurred in these cells, such as reduced cyclin B expression and altered phosphorylation of CDK1, which could prevent proper formation of nuclear cyclin B-CDK1 complexes, resulting in G_2 block (50–52).

Senescence is identified by finite number of doublings that primary cells can undergo in culture, along with expression of certain biomarkers, such as SAB (53). Little is understood about the origin and function of SAB, which is thought to be an alternatively spliced isoform of lysosomal β-galactosidase, with increased activity in senescent cells (54). The finding of increased SAB activity in CNE-1 cells after adv.*p16* infection indicates that a subset of the treated population has entered senescence (Fig. 5). This is consistent with previous studies showing that adenoviral-mediated *p16* overexpression can induce premature senescence (30, 34).

Although apoptosis was not a major feature of p16-mediated cytotoxicity for the CNE-1 cells, others have reported that exogenous *p16* can induce significant tumor cell apoptosis (55). In a recent study of several human cancer cell lines, stable transfection of *p16* was shown to restore anoikis (56), the induction of apoptosis due to loss of anchorage to surrounding tissues. The observation that exogenous *p16* expression can also down-regulate the anti-apoptotic protein bcl-2 (19) further strengthens the association between *p16* and apoptosis.

We observed that adv.*p16* (alone or in combination with RT) led to significant necrosis (~20%), consistent with other reports for prostate (16) and ovarian cancer models (36). Although *p16*-induced necrosis has been described in many studies, the mechanism remains to be elucidated. In the final analysis, we have examined several potential modes of cytotoxicity, including apoptosis, necrosis, arrest, and senescence. The arithmetic sum of all of these data will still not fully account for the 99.9% clonogenic death of CNE-1 cells after infection with adv.*p16* (25 pfu/cell in Fig. 3). This suggests at least two possibilities. The first is that there are additional modes of cellular damage, which result in failure of reproductive potential in cancer cells. A second consideration would be that arithmetic summation

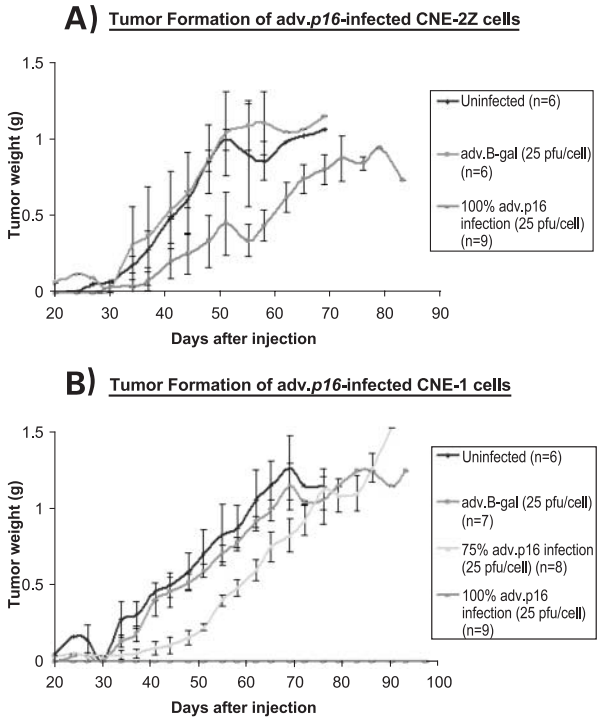

Figure 8. Inhibition of NPC tumor growth in SCID mice. Twenty-four hours after CNE-1 and CNE-2Z cells were treated [mock infection, adv.β-*gal* (25 pfu/cell), or adv.*p16* (25 pfu/cell)], they were trypsinized, counted, and injected into SCID mice. Approximately 4×10^6 cells in 100 μl of PBS were injected i.m. into the left calf of each mouse. Animals were then monitored for tumor formation and growth. Each *data point* represents mean tumor weight of three independent experiments; *bars,* SE. The number in parentheses indicates the number of mice in each experimental group. **A,** CNE-2Z cells; **B,** CNE-1 cells.

Downloaded from http://aacrjournals.org/mct/article-pdf/2/10/961/1864970/961-969.pdf by guest on 05 October 2024

of these assays is an oversimplification of the clonogenic data, particularly when the former assays are short-term assessments (within 48 h of infection), whereas the clonogenic data are derived after 10–14 days of incubation.

Several studies have documented loss of tumorigenic potential for various human cancers *in vivo* following *p16* gene transfer (20, 21, 29). In particular, Wang *et al.* (21) demonstrated significant growth suppression by stably transfecting *p16* into a NPC cell line HK-1, which harbors mutant *p16* (12). Their *in vivo* study also indicated that *p16*-expressing NPC transfectants failed to form tumors in athymic nude mice (21). In our study, tumorigenicity experiments revealed that adv.*p16*-treated CNE-1 cells failed to establish tumors, in contrast to the CNE-2Z cells. However, for this treatment to completely prevent tumor formation, 100% of the cells need to be infected. Even if 75% of the CNE-1 cells were infected, tumors will still form (Fig. 8B). This underscores the current challenge of cancer gene therapy whereby the vast majority of cancer cells need to express the therapeutic gene before complete tumor eradication can be achieved.

In summary, this study demonstrated that adv.*p16* therapy is significantly cytotoxic to NPC cells that harbor low levels of endogenous p16 protein. The mechanism of p16 cytotoxicity appears to be multimodal, with necrosis, G_1 arrest, and senescence being most significant. RT provided an additive therapeutic benefit to adv.*p16* for both cell lines by inducing G_2 arrest and apoptosis. Overall, given the exquisite sensitivity of CNE-1 cells to adv.*p16* gene transfer, and the absence of p16 expression in the majority of primary NPC (9, 57), the therapeutic potential of this strategy warrants further detailed investigations.

References

1. Yu, M. C., and Yuan, J. M. Epidemiology of nasopharyngeal carcinoma. Semin. Cancer Biol., *12:* 421–429, 2002.

2. Altun, M., Fandi, A., Dupuis, O., Cvitkovic, E., Krajina, Z., and Eschwege, F. Undifferentiated nasopharyngeal cancer (UCNT): current diagnostic and therapeutic aspects. Int. J. Radiat. Oncol. Biol. Phys., *32:* 859–877, 1995.

3. Hsu, J. L. and Glaser, S. L. Epstein-Barr virus-associated malignancies: epidemiologic patterns and etiologic implications. Crit. Rev. Oncol. Hematol., *34:* 27–53, 2000.

4. Lee, N., Xia, P., Quivey, J. M., Sultanem, K., Poon, I., Akazawa, C., Akazawa, P., Weinberg, V., and Fu, K. K. Intensity-modulated radiotherapy in the treatment of nasopharyngeal carcinoma: an update of the UCSF experience. Int. J. Radiat. Oncol. Biol. Phys., *53:* 12–22, 2002.

5. Chow, E., Payne, D., O'Sullivan, B., Pintilie, M., Liu, F. F., Waldron, J., Warde, P., and Cummings, B. Radiotherapy alone in patients with advanced nasopharyngeal cancer: comparison with an intergroup study. Is combined modality treatment really necessary? Radiother. Oncol., *63:* 269–274, 2002.

6. Lo, K. W. and Huang, D. P. Genetic and epigenetic changes in nasopharyngeal carcinoma. Semin. Cancer Biol., *12:* 451–462, 2002.

7. Serrano, M. The tumor suppressor protein p16INK4a. Exp. Cell Res., *237:* 7–13, 1997.

8. Gulley, M. L., Nicholls, J. M., Schneider, B. G., Amin, M. B., Ro, J. Y., and Geradts, J. Nasopharyngeal carcinomas frequently lack the p16/MTS1 tumor suppressor protein but consistently express the retinoblastoma gene product. Am. J. Pathol., *152:* 865–869, 1998.

9. Shibosawa, E., Tsutsumi, K., Koizuka, I., Hoshikawa, M., and Takakuwa, T. Absence of nuclear p16 from Epstein-Barr virus-associated undifferentiated nasopharyngeal carcinomas. Laryngoscope, *110:* 93–97, 2000.

10. Makitie, A., MacMillan, C., Ho, J., Shi, W., Pintilie, M., O'Sullivan, B., Payne, D., Gullane, P., and Liu, F-F. p16 alteration in human nasopharyngeal carcinoma. *In:* Canadian Association of Radiation Oncologists, Toronto, Ontario, October 25–27, 2002.

11. Lo, K-W., Cheung, S-T., Leong, S-F., van Hasselt, A., Tsang, Y-S., Mak, K-F., Chung, Y-F., Woo, J., Lee, J. C. K., and Huang, D. Hypermethylation of the *p16* gene in nasopharyngeal carcinoma. Cancer Res., *56:* 2721–2725, 1996.

12. Lo, K. W., Huang, D. P., and Lau, K. M. p16 gene alterations in nasopharyngeal carcinoma. Cancer Res., *55:* 2039–2043, 1995.

13. Rocco, J. W., Li, D., Liggett, W. H., Jr., Duan, L., Saunders, J. K., Jr., Sidransky, D., and O'Malley, B. W., Jr. p16INK4A adenovirus-mediated gene therapy for human head and neck squamous cell cancer. Clin. Cancer Res., *4:* 1697–1704, 1998.

14. Campbell, I., Magliocco, A., Moyama, T., Zheng, C., and Xiang, J. Adenovirus-mediated p16INK4 gene transfer significantly suppresses human breast cancer growth. Cancer Gene Ther., *7:* 1270–1278, 2000.

15. Naruse, I., Heike, Y., Hama, S., Mori, M., and Saijo, N. High concentrations of recombinant adenovirus expressing p16 gene induces apoptosis in lung cancer cell lines. Anticancer Res., *18:* 4275–4282, 1998.

16. Allay, J. A., Steiner, M. S., Zhang, Y., Reed, C. P., Cockroft, J., and Lu, Y. Adenovirus p16 gene therapy for prostate cancer. World J. Urol., *18:* 111–120, 2000.

17. Kobayashi, S., Shirasawa, H., Sashiyama, H., Kawahira, H., Kaneko, K., Asano, T., and Ochiai, T. P16INK4a expression adenovirus vector to suppress pancreas cancer cell proliferation. Clin. Cancer Res., *5:* 4182–4185, 1999.

18. Kim, M., Katayose, Y., Rojanala, L., Shah, S., Sgagias, M., Jang, L., Jung, Y. J., Lee, S. H., Hwang, S. G., and Cowan, K. H. Induction of apoptosis in p16INK4A mutant cell lines by adenovirus-mediated overexpression of p16INK4A protein. Cell Death Differ., *7:* 706–711, 2000.

19. Kataoka, M., Wiehle, S., Spitz, F., Schumacher, G., Roth, J. A., and Cristiano, R. J. Down-regulation of bcl-2 is associated with p16INK4-mediated apoptosis in non-small cell lung cancer cells. Oncogene, *19:* 1589–1595, 2000.

20. Schreiber, M., Muller, W. J., Singh, G., and Graham, F. L. Comparison of the effectiveness of adenovirus vectors expressing cyclin kinase inhibitors p16INK4A, p18INK4C, p19INK4D, p21(WAF1/CIP1) and p27KIP1 in inducing cell cycle arrest, apoptosis and inhibition of tumorigenicity. Oncogene, *18:* 1663–1676, 1999.

21. Wang, G. L., Lo, K. W., Tsang, K. S., Chung, N. Y., Tsang, Y. S., Cheung, S. T., Lee, J. C., and Huang, D. P. Inhibiting tumorigenic potential by restoration of p16 in nasopharyngeal carcinoma. Br. J. Cancer, *81:* 1122–1126, 1999.

22. Zeng, Y. Establishment of an epithelioid cell line and a fusiform cell line from a patient with nasopharyngeal carcinoma. Sci. Sin., *21:* 127, 1978.

23. Sizhong, Z., Xiukung, G., and Zeng, Y. Cytogenetic studies on an epithelial cell line derived from poorly differentiated nasopharyngeal carcinoma. Int. J. Cancer, *31:* 587–590, 1983.

24. Zhang, W. W., Alemany, R., Wang, J., Koch, P. E., Ordonez, N. G., and Roth, J. A. Safety evaluation of Ad5CMV-p53 *in vitro* and *in vivo*. Hum. Gene Ther., *6:* 155–164, 1995.

25. Li, J. H., Lax, S. A., Kim, J., Klamut, H., and Liu, F. F. The effects of combining ionizing radiation and adenoviral p53 therapy in nasopharyngeal carcinoma. Int. J. Radiat. Oncol. Biol. Phys., *43:* 607–616, 1999.

26. Li, J. H., Li, P., Klamut, H., and Liu, F. F. Cytotoxic effects of Ad5CMV-p53 expression in two human nasopharyngeal carcinoma cell lines. Clin. Cancer Res., *3:* 507–514, 1997.

27. Schumer, M., Colombel, M. C., Sawczuk, I. S., Gobe, G., Connor, J., O'Toole, K. M., Olsson, C. A., Wise, G. J., and Buttyan, R. Morphologic, biochemical, and molecular evidence of apoptosis during the reperfusion phase after brief periods of renal ischemia. Am. J. Pathol., *140:* 831–838, 1992.

28. Lax, S. A., Chia, M. C., Busson, P., Klamut, H. J., and Liu, F. F. Adenovirus-p53 gene therapy in human nasopharyngeal carcinoma xenografts. Radiother. Oncol., *61:* 309–312, 2001.

29. Jin, X., Nguyen, D., Zhang, W. W., Kyritsis, A. P., and Roth, J. A. Cell cycle arrest and inhibition of tumor cell proliferation by the p16INK4 gene mediated by an adenovirus vector. Cancer Res., *55:* 3250–3253, 1995.

30. Calbo, J., Marotta, M., Cascallo, M., Roig, J. M., Gelpi, J. L., Fueyo, J., and Mazo, A. Adenovirus-mediated wt-p16 reintroduction induces cell

Downloaded from http://aacrjournals.org/mct/article-pdf/2/10/961/1864970/961-969.pdf by guest on 05 October 2024

cycle arrest or apoptosis in pancreatic cancer. Cancer Gene Ther., *8:* 740 – 750, 2001.

31. Brenner, A. J., Stampfer, M. R., and Aldaz, C. M. Increased p16 expression with first senescence arrest in human mammary epithelial cells and extended growth capacity with p16 inactivation. Oncogene, *17:* 199 – 205, 1998.

32. Dai, C. Y. and Enders, G. H. p16 INK4a can initiate an autonomous senescence program. Oncogene, *19:* 1613 – 1622, 2000.

33. Jarrard, D. F., Sarkar, S., Shi, Y., Yeager, T. R., Magrane, G., Kinoshita, H., Nassif, N., Meisner, L., Newton, M. A., Waldman, F. M., and Reznikoff, C. A. p16/pRb pathway alterations are required for bypassing senescence in human prostate epithelial cells. Cancer Res., *59:* 2957 – 2964, 1999.

34. Steiner, M. S., Zhang, Y., Farooq, F., Lerner, J., Wang, Y., and Lu, Y. Adenoviral vector containing wild-type p16 suppresses prostate cancer growth and prolongs survival by inducing cell senescence. Cancer Gene Ther., *7:* 360 – 372, 2000.

35. Uhrbom, L., Nister, M., and Westermark, B. Induction of senescence in human malignant glioma cells by p16INK4A. Oncogene, *15:* 505 – 514, 1997.

36. Wolf, J. K., Kim, T. E., Fightmaster, D., Bodurka, D., Gershenson, D. M., Mills, G., and Wharton, J. T. Growth suppression of human ovarian cancer cell lines by the introduction of a p16 gene via a recombinant adenovirus. Gynecol. Oncol., *73:* 27 – 34, 1999.

37. Modesitt, S. C., Ramirez, P., Zu, Z., Bodurka-Bevers, D., Gershenson, D., and Wolf, J. K. *In vitro* and *in vivo* adenovirus-mediated p53 and p16 tumor suppressor therapy in ovarian cancer. Clin. Cancer Res., *7:* 1765 – 1772, 2001.

38. Ghaneh, P., Greenhalf, W., Humphreys, M., Wilson, D., Zumstein, L., Lemoine, N. R., and Neoptolemos, J. P. Adenovirus-mediated transfer of p53 and p16(INK4a) results in pancreatic cancer regression *in vitro* and *in vivo*. Gene Ther., *8:* 199 – 208, 2001.

39. Qi, V., Weinrib, L., Ma, N., Li, J. H., Klamut, H., and Liu, F. F. Adenoviral *p53* gene therapy promotes heat-induced apoptosis in a nasopharyngeal carcinoma cell line. Int. J. Hyperthermia, *17:* 38 – 47, 2001.

40. Liu, T-J., El-Naggar, A., McDonnell, T., Steck, K., Wang, M., Taylor, D., and Clayman, G. L. Apoptosis induction mediated by wild-type *p53* adenoviral gene transfer in squamous cell carcinoma of the head and neck. Cancer Res., *55:* 3117 – 3122, 1995.

41. Katayose, D., Gudas, J., Nguyen, H., Srivastava, S., Cowan, K., and Seth, P. Cytotoxic effects of adenovirus-mediated wild-type p53 protein expression in normal and tumor mammary epithelial cells. Clin. Cancer Res., *1:* 889 – 897, 1995.

42. Cirielli, C., Riccioni, T., Yang, C., Pili, R., Gloe, T., Chang, J., Inyaku, K., Passaniti, A., and Capogrossi, M. Adenovirus-mediated gene transfer of wild-type p53 results in melanoma cell apoptosis *in vitro* and *in vivo*. Int. J. Cancer, *63:* 673 – 679, 1995.

43. Yang, C., Cirielli, C., Capogrossi, M., and Passaniti, A. Adenovirus-mediated wild-type *p53* expression induces apoptosis and suppresses tumorigenesis of prostatic tumor cells. Cancer Res., *55:* 4120 – 4213, 1995.

44. Fang, X., Jin, X., Xu, H. J., Liu, L., Peng, H. Q., Hogg, D., Roth, J. A., Yu, Y., Xu, F., Bast, R. C., Jr., and Mills, G. B. Expression of p16 induces transcriptional down-regulation of the RB gene. Oncogene, *16:* 1 – 8, 1998.

45. Morris, E. J. and Dyson, N. J. Retinoblastoma protein partners. Adv. Cancer Res., *82:* 1 – 54, 2001.

46. Lukas, J., Parry, D., Aagaard, L., Mann, D. J., Bartkova, J., Strauss, M., Peters, G., and Bartek, J. Retinoblastoma-protein-dependent cell-cycle inhibition by the tumour suppressor p16. Nature, *375:* 503 – 506, 1995.

47. Matsumura, Y., Yamagishi, N., Miyakoshi, J., Imamura, S., and Takebe, H. Increase in radiation sensitivity of human malignant melanoma cells by expression of wild-type p16 gene. Cancer Lett., *115:* 91 – 96, 1997.

48. Miyakoshi, J., Kitagawa, K., Yamagishi, N., Ohtsu, S., Day, R. S., 3rd, and Takebe, H. Increased radiosensitivity of p16 gene-deleted human glioma cells after transfection with wild-type p16 gene. Jpn. J. Cancer Res., *88:* 34 – 38, 1997.

49. Chow, L. S., Wang, X., Kwong, D. L., Sham, J. S., Tsao, S. W., and Nicholls, J. M. Effect of p16INK4a on chemosensitivity in nasopharyngeal carcinoma cells. Int. J. Oncol., *17:* 135 – 140, 2000.

50. Maity, A., McKenna, W. G., and Muschel, R. J. The molecular basis for cell cycle delays following ionizing radiation: a review. Radiother. Oncol., *31:* 1 – 13, 1994.

51. Smeets, M. F., Mooren, E. H., and Begg, A. C. The effect of radiation on G2 blocks, cyclin B expression and cdc2 expression in human squamous carcinoma cell lines with different radiosensitivities. Radiother. Oncol., *33:* 217 – 227, 1994.

52. Metting, N. F. and Little, J. B. Transient failure to dephosphorylate the cdc2-cyclin B1 complex accompanies radiation-induced G2-phase arrest in HeLa cells. Radiat. Res., *143:* 286 – 292, 1995.

53. Dimri, G. P., Lee, X., Basile, G., Acosta, M., Scott, G., Roskelley, C., Medrano, E. E., Linskens, M., Rubelj, I., Pereira-Smith, O., *et al.* A biomarker that identifies senescent human cells in culture and in aging skin *in vivo*. Proc. Natl. Acad. Sci. USA, *92:* 9363 – 9367, 1995.

54. Morreau, H., Galjart, N. J., Gillemans, N., Willemsen, R., van der Horst, G. T., and d'Azzo, A. Alternative splicing of β-galactosidase mRNA generates the classic lysosomal enzyme and a β-galactosidase-related protein. J. Biol. Chem., *264:* 20655 – 20663, 1989.

55. Rocco, J. W. and Sidransky, D. p16(MTS-1/CDKN2/INK4a) in cancer progression. Exp. Cell Res., *264:* 42 – 55, 2001.

56. Plath, T., Detjen, K., Welzel, M., von Marschall, Z., Murphy, D., Schirner, M., Wiedenmann, B., and Rosewicz, S. A novel function for the tumor suppressor p16(INK4a): induction of anoikis via upregulation of the α(5)β(1) fibronectin receptor. J. Cell Biol., *150:* 1467 – 1478, 2000.

57. Gulley, M. L., Burton, M. P., Allred, D. C., Nicholls, J. M., Amin, M. B., Ro, J. Y., and Schneider, B. G. Epstein-Barr virus infection is associated with p53 accumulation in nasopharyngeal carcinoma. Hum. Pathol., *29:* 252 – 259, 1998.

Downloaded from http://aacrjournals.org/mct/article-pdf/2/10/961/1864970/961-969.pdf by guest on 05 October 2024